Eduard E. de Lange, MD
John P. Mugler III, PhD
James R. Brookeman, PhD
Jack Knight-Scott, PhD
Jonathon D. Truwit, MD
C. David Teates, MD
Thomas M. Daniel, MD
Paul L. Bogorad, PhD
Gordon D. Cates, PhD

Index terms:
Helium
Lung, MR, 60.12143
Magnetic resonance (MR), contrast enhancement, 60.121412, 60.12143
Magnetic resonance (MR), nuclei other than H, 60.121412, 60.12147

Radiology 1999; 210:851–857

Abbreviation:
FLASH = fast low-angle shot

[1] From the Departments of Radiology (E.E.d.L., J.P.M., J.R.B., J.K.S., C.D.T.), Internal Medicine (J.D.T.), and Surgery (T.M.D.), University of Virginia Health Sciences Center, Box 170, 1000 Lee St, Charlottesville, VA 22908; Magnetic Imaging Technologies, Durham, NC (P.L.B.); and the Department of Physics, Princeton University, Princeton, NJ (G.D.C.). From the 1998 RSNA scientific assembly. Received February 25, 1998; revision requested April 27; revision received July 21; accepted September 28. Supported in part by National Institutes of Health grant 1R43-HL59022-01; the University of Virginia Pratt Fund; the Dean of the Medical School, Robert M. Carey, MD; and Siemens Medical Systems. **Address reprint requests to** E.E.d.L.

Author contributions:
Guarantors of integrity of entire study, E.E.d.L., J.P.M., J.R.B.; study concepts and design, E.E.d.L., J.P.M., J.R.B., T.M.D.; definition of intellectual content, E.E.d.L.; literature research, E.E.d.L., J.P.M., J.R.B.; clinical studies, E.E.d.L., J.D.T., T.M.D.; experimental studies, J.P.M., J.R.B., P.L.B., J.K.S., G.D.C.; data acquisition, E.E.d.L., J.P.M., J.R.B., C.D.T., P.L.B., J.K.S., G.D.C.; data analysis, E.E.d.L., J.P.M., J.R.B.; manuscript preparation, E.E.d.L.; manuscript editing, E.E.d.L., J.P.M., J.R.B.; manuscript review, J.D.T., C.D.T., T.M.D.

Lung Air Spaces: MR Imaging Evaluation with Hyperpolarized ^{3}He Gas[1]

Thirty-two magnetic resonance imaging examinations of the lungs were performed in 16 subjects after inhalation of 1–2 L of helium 3 gas that was laser polarized to 10%–25%. The distribution of the gas was generally uniform, with visualization of the fissures in most cases. Ventilation defects were demonstrated in smokers and in a subject with allergies. The technique has potential for evaluating small airways disease.

Recent developments in magnetic resonance (MR) imaging in animals and human subjects have shown that images of the air spaces of the lung can be obtained after inhalation of hyperpolarized noble gases, including helium 3 and xenon 129 (1–10). The emergence of this technique is remarkable, as until these developments, visualization of the alveolar and bronchial spaces with use of conventional hydrogen 1 MR imaging was not possible because of the low concentration of ^{1}H nuclei from water vapor providing too weak a signal for successful imaging. Until now, clinical imaging of the lung parenchyma and ventilation was performed with chest radiography, x-ray computed tomography with or without inhalation of xenon gas as a contrast agent, or ventilation scintigraphy with inhalation of radioactive gases and aerosols. However, each technique has its problems, such as limitations in sensitivity or spatial resolution, and they involve the use of ionizing radiation with associated risks. Thus, an advantage of MR imaging with noble gases is that the lung spaces can be evaluated without exposure to radiation.

In this study, we evaluated the potential application of lung MR imaging with hyperpolarized ^{3}He. Helium was used because it has a much greater magnetic moment than ^{129}Xe and depolarizes more slowly. In addition, ^{3}He can be inhaled in relatively large quantities without substantial risk as it is not absorbed by the tissues of the lung. Furthermore, there are no known serious side effects associated with inhalation of helium gas, on the basis of experience in deep-sea divers who typically use much larger volumes and concentrations than are used with MR imaging of the lungs (6). The promising initial imaging results and inherent safety of ^{3}He coupled with an emerging commercial supply of polarized ^{3}He gas for the clinical environment makes further investigation of this contrast agent a desirable endeavor.

The purpose of our study was twofold. First, we assessed the ability to manage and operate a prototypic ^{3}He gas polarizer in a clinical environment to routinely and reliably deliver polarized gas for imaging subjects in a 1.5-T MR imager. The MR imager included a broad-band spectroscopy option modified, in a straightforward manner, to operate at the resonant frequency of 48 MHz for ^{3}He. Second, we investigated the application of hyperpolarized ^{3}He MR imaging in a variety of subjects to assess the range of typical image features and variants that can be expected, as a foundation for developing an understanding of the capabilities of ^{3}He imaging for depiction and evaluation of lung air space anatomy, ventilatory function, and pathologic conditions.

Materials and Methods

We performed 32 MR examinations of the lungs in 16 subjects (10 men and six women; age range, 20–71 years; mean age, 37.8 years) after inhalation of hyperpolarized ^{3}He gas. Thirteen were healthy subjects with no known lung disease or smoking history. The remaining three subjects had a history of smoking. One was a middle-aged heavy smoker who was otherwise healthy. Another, who was

middle-aged and used to be a heavy smoker, had been treated in the past for lung disease related to smoking (''emphysema''), but he had no symptoms at the time of the study and was not taking medications. The third was a 71-year-old man with a clinical diagnosis of severe, smoking-related emphysema, whose forced expiratory volume in 1 second, or FEV_1, was 41% (predicted).

Gas Preparation and Delivery

Polarization of the ^{3}He gas was performed with a prototypic system (Magnetic Imaging Technologies, Durham, NC) with use of the method of collisional spin exchange between ^{3}He and an optically pumped rubidium vapor (2). For this process, ^{3}He is enclosed in a cylindrical glass chamber, which is in a low magnetic field (approximately 10 G), at a pressure of approximately 8 atm. At this pressure, the rubidium absorption profile is broadened to provide an improved match to the broad-beam profile of the diode-array laser, thereby giving an increased light absorption efficiency. This glass chamber also contains trace amounts of rubidium and molecular nitrogen (N_2 serves as a buffer gas to reduce optical deexcitation of the rubidium). Circularly polarized laser light, tuned to the D1 resonance of rubidium, illuminates the glass chamber which is heated to 200°C to produce a rubidium vapor density of roughly 1 ppm of the ^{3}He density. Absorption of the laser light produces a high electronic polarization in the rubidium atoms by means of optical pumping (Fig 1). Subsequent gas collisions between the rubidium and ^{3}He atoms then transfer some of this polarization to the ^{3}He nuclei. The collisional spin exchange is very slow, with a typical time constant on the order of hours. After polarizing for 6–8 hours, the chamber is cooled to room temperature, which causes most of the vapor to condense out onto the walls of the cell so that an infinitesimal amount ($<$0.01 μg) of rubidium is introduced into the subject breathing the hyperpolarized ^{3}He gas. As an additional precaution, the ^{3}He gas is passed through a 0.2-μm filter (Gelman Sciences, Ann Arbor, Mich) to ensure removal of any rubidium droplets from the gas stream. The prototypic polarization system is relatively compact, requiring approximately 30 sq ft (2.8 m^2) for siting, including access for operation and service. The only special requirements for operation include a 220-V power source and compressed air.

For each experiment, the ^{3}He gas was polarized for 6–8 hours, yielding polarizations of 10%–25%. The polarization was measured with an on-board nuclear MR polarimeter, which was calibrated for each glass cell. The polarimeter compared the nuclear MR signal from the hyperpolarized gas with that for thermal equilibrium ^{1}H in a water sample. When maximum polarization was achieved, the gas was transferred from the polarizer into a small (1- or 2-L) plastic bag equipped with a short tube and a hand-operated valve. The bag with the ^{3}He gas at 1 atm pressure was then transported to the imager, where the subject was already positioned supine in the magnet. Immediately before commencing the imaging, the bag was given to the subject to inhale the gas through the short tube after opening the valve. In each case, the subject inhaled the gas quickly, typically in less than 5 seconds. Initial experiments were performed with relatively large volumes (2 L) of the gas. As the gas polarization increased due to refinements of the polarization system and as our pulse sequence techniques were optimized, the volumes of gas were reduced. In 22 of the 32 studies, 1 L of the gas was given; in the rest, the amount varied up to 2 L. MR imaging was performed with breath holding commencing immediately after inhalation of the gas.

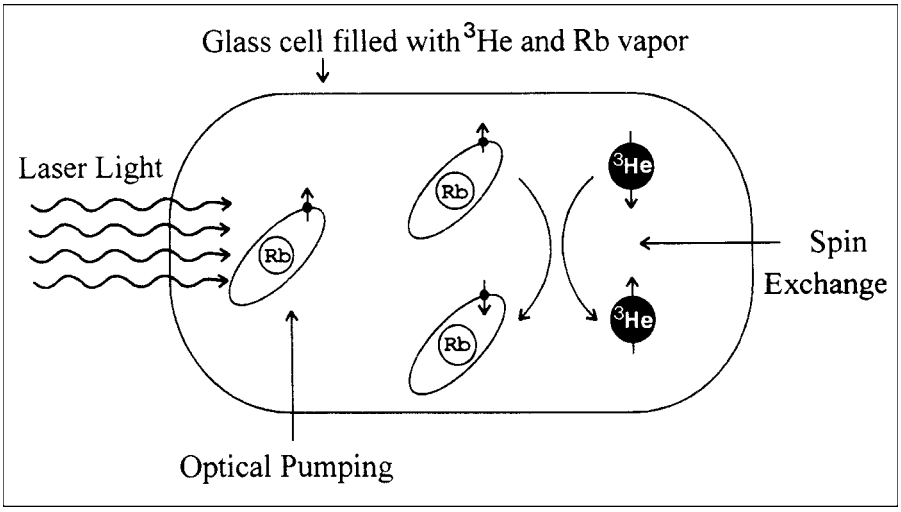

Figure 1. Schematic depicts optical pumping and spin exchange. The glass cell is filled with ^{3}He gas and a small quantity of rubidium. Heating of the cell produces rubidium vapor. When the mixture is illuminated by laser light, absorption of the light causes high electronic polarization in the rubidium atoms by means of the process called ''optical pumping.'' When the polarized rubidium atoms collide with the ^{3}He atoms, the polarization is transferred to the ^{3}He nuclei. Transfer of the polarization is referred to as ''spin exchange.''

Figure 2. Photograph of the prototypic, close-fitting, 48-MHz radio-frequency coil (arrow) used for acquisition of the hyperpolarized ^{3}He images. The coil is a Helmholtz pair with an element diameter of 28.5 cm, covering the extent of the lungs in most subjects. One coil element is above the subject and the other beneath. Separation between the elements is adjusted for the chest size of the subject.

Imaging Equipment

The studies were performed by using a commercial 1.5-T whole-body imager (Magnetom Vision; Siemens Medical Systems, Iselin, NJ) modified to operate at 48 MHz by the addition of a broad-band radio-frequency amplifier. A prototypic, close-fitting, 48-MHz radio-frequency coil was used for data acquisition (Fig 2). This coil was a Helmholtz pair with an element diameter of 28.5 cm, which was large enough to cover the extent of the

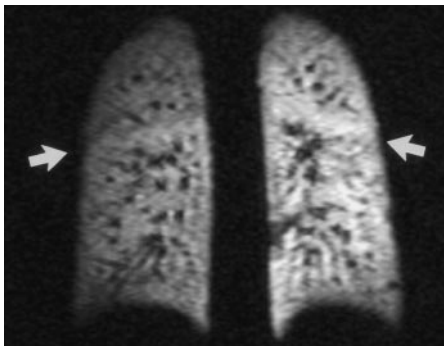

a.

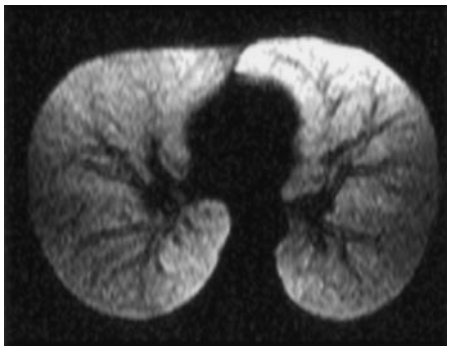

b.

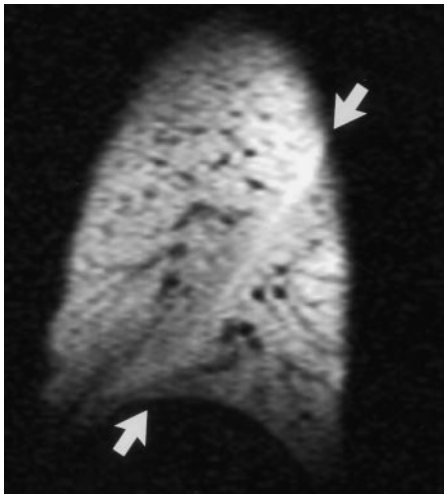

c.

Figure 3. **(a)** Coronal, **(b)** axial, and **(c)** sagittal ^{3}He MR images (two-dimensional FLASH) of the lungs of a healthy subject. Each image was obtained in a single breath hold after inhalation of 1 L of ^{3}He gas. There is uniform distribution of the gas, which displays high signal intensity. The low-intensity structures are the normal blood vessels. The major fissure (arrows) of the lung is seen in **a** and **c**. The images were obtained with a 28.5-cm Helmholtz coil. The high signal intensity of the anterior and posterior aspects of the lung shown in **b** and **c**, respectively, is caused by the proximity of the coil elements to the chest wall.

lungs in most subjects. The coil operated in a transmit-receive mode and was positioned with one coil element beneath the subject and the other coil element above. The separation between the elements was adjusted for the chest size of the subject.

Pulse Sequence Techniques

In 26 of the 32 imaging studies, a gradient-echo, two-dimensional, fast low-angle shot (FLASH) sequence was used with the following typical parameters: repetition time, 13.3 msec (section-sequential acquisition) or 120–145 msec (section-interleaved acquisition); echo time, 5.4 msec; flip angle, 5°–10°; matrix, 64–128 × 256; field of view, 40–55 cm; section thickness, 8–20 mm; and one signal acquired. Nine to 24 sections were collected during a 15–22-second breath hold, and the acquisition time ranged from 0.9 to 1.7 seconds per image. Initial experiments were performed with relatively thick (2-cm) sections and low in-plane resolution. With improvements in gas polarization and optimization of the pulse sequence techniques, the section thickness and in-plane resolution were reduced to values typical for breath-hold, body-coil proton imaging. The most common imaging plane chosen was coronal because this orientation required acquisition of the fewest sections of a given thickness to cover the chest. In some studies, other orientations were used to explore the depiction of the lungs in these planes. The images were obtained in coronal orientation in 21 studies, axial in two, and sagittal in three. In the remaining six studies, a two-dimensional, interleaved echo-planar, gradient-echo pulse sequence was used that provided 15–25 image sections in 4.9–9.7 seconds (acquisition time, 0.32 or 0.38 seconds per image). In five of the six studies, the images were obtained in coronal orientation; in one study, sagittal. Echo train lengths of three and five were used, and the typical pulse sequence parameters were repetition time, 10.3 or 15.2 msec; echo time, 5.3 or 8.0 msec; matrix, 102 × 256 or 100 × 256 for echo train lengths of three and five, respectively; flip angle, 15°–20°; field of view, 35 × 56 cm; section thickness, 10 mm; and one signal acquired. Pertinent features of the interleaved echo-planar pulse sequences included (*a*) a separate navigator echo just after each excitation radio-frequency pulse to permit correction of the change in signal amplitude with excitation number, (*b*) echo-time shifting to minimize artifacts from off-resonance signal sources, and (*c*) corrections for gradient and timing imperfections on the basis of a non–phase-encoded image. To outline the chest, conventional ^{1}H MR images were obtained in 11 of the 32 studies.

The MR protocols were approved by our institutional review board, and informed consent was obtained from all participants. Throughout each study, the subject's heart rate and blood oxygen saturation level were monitored. All procedures were supervised by a physician.

Image Review

The images were reviewed in consensus by two experienced radiologists (E.E.d.L., C.D.T.) who were blinded to any information about the subjects with respect to their age, sex, and clinical data, if any. One of the observers had considerable experience in MR imaging and relatively little experience in scintigraphy, and the second observer had considerable experience in ventilation scintigraphy and relatively little experience in MR imaging. They assessed together (at the same time) whether the distribution of the inhaled ^{3}He gas in the lungs, the visualization of the trachea and first degree bronchi, the coverage of the two lungs by the radio-frequency coil, and the overall diagnostic quality of the images was good, moderate, or poor. In addition, assessments were made whether the lung fissures were visualized over their entire extent, partially, or not at all, and whether there were large, moderate, or small ventilation defects. Assessments were also made as to whether there were artifacts caused by motion of the heart or great vessels that were substantial enough to interfere with image interpretation or whether these artifacts were mild or absent. The reviewers also evaluated in consensus whether there were any apparent differences in image quality and depiction of the lungs between the two-dimensional FLASH and interleaved echo-planar sequences. Subsequently, to test the ability to assess pathologic findings in a reproducible manner on hyperpolarized ^{3}He images, the two reviewers were asked, several weeks after the consensus review, to score independently the severity of lung abnormalities (ie, ventilation defects) for each of the 32 studies. Grading was performed with a continuous 10-point scale in which the score of 1 represented no disease and the score of 10 represented severe disease.

Statistical Analysis

The degree of association between the two independent evaluations of the sever-

ity of lung defects was assessed with the Spearman rank correlation. This correlation measures the degree to which the reviewers agree on the ordering of the images from the least to the most severe lung defects.

Results

Patient Monitoring

Monitoring of the blood oxygen saturation levels during inhalation of the hyperpolarized gas did not show a substantial (>5%) change in the levels of either the healthy subjects or those with a history of smoking. In addition, all participants were able to inhale the gas without difficulty and to hold their breath during acquisition of the data.

Imaging Studies

The distribution of the gas was rated as good in 24 of the 32 studies (Fig 3), moderate in six, and poor in two. The lung fissures were seen over their entire extent in six cases, over a large extent in 12, and over a small extent in six. The fissures could not be identified in the remaining eight studies. The trachea and first bronchi were visualized well in one case, relatively well in eight cases, and poorly in 13, and were not seen in 10. Defects were large in three studies, moderate in four, and small in three (Fig 4). The defects were most extensive in the patient with severe emphysema and corresponded to defects seen at xenon 133 ventilation (wash-in) scintigraphy several months earlier (Fig 5). In one of the healthy subjects, a few small defects were seen (Fig 6a); at ^{3}He imaging 1 week later, the defects had disappeared but several new defects, including a large one, were seen in different areas of the lungs (Fig 6b). Upon further questioning, the volunteer indicated that she had a history of asthma and had been experiencing mild seasonal allergies without noticeable pulmonary symptoms. At repeat follow-up ^{3}He MR examination 1 week after the second study, the defects had disappeared and all symptoms had subsided (Fig 6c). In all healthy subjects, the gas was noted to be present in all areas of the lungs including those most peripheral, Iin all cases with ventilation defects, the noninvolved portions of the lungs were well visualized. This indicates that the single breath hold of the hyperpolarized gas was sufficient to fill all functioning lung spaces. Motion artifacts (pulsation artifacts from the heart or great vessels against the lung) that interfered with image interpretation were substantial in three studies, mild in two, and absent in the remaining 27. Coverage of the 28.5-cm Helmholtz coil was good in 24 studies, moderate in seven, and poor in one study. The overall diagnostic quality was rated as good for 28 studies, moderate for three, and poor for one study, which was performed at the beginning of our experiments. No apparent differences in image quality and lung depiction were noted with the two-dimensional FLASH versus the interleaved echo-planar sequences (Fig 7).

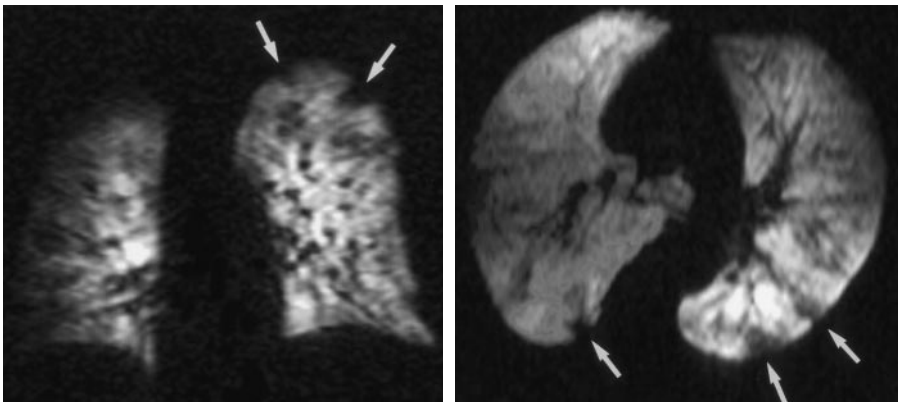

a. **b.**

Figure 4. **(a)** Coronal and **(b)** axial lung ^{3}He MR images (two-dimensional FLASH) in a middle-aged heavy smoker. There are multiple small ventilation defects (several indicated with arrows) in both lungs. Note that the outer (lateral) edge of the right lung is only faintly visible in **a** due to incomplete coverage of the chest by the 28.5-cm Helmholtz coil. The coil was repositioned before **b** was acquired.

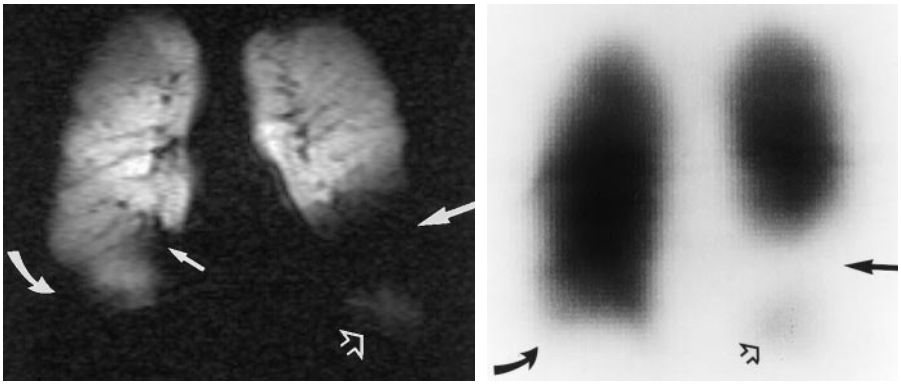

a. **b.**

Figure 5. **(a)** Coronal MR image (two-dimensional FLASH) in a 71-year-old patient with severe emphysema was obtained immediately after inhalation of 1 L of hyperpolarized ^{3}He gas. A very large ventilation defect is seen in the lower aspect of the left lung (large straight arrow), and faint signal intensity (open arrow) from the gas is seen at the lung base adjacent to the hemidiaphragm. A large defect is also present at the right base (curved arrow) and a small defect more medially (small straight arrow). **(b)** Ventilation (wash-in) ^{133}Xe scintigraphic image shows similar bilateral defects (curved and straight arrows) and faint uptake of ^{133}Xe activity (open arrow) adjacent to the left diaphragm. The small defect in the medial aspect of the lower right lung (small straight arrow in **a**) is difficult to appreciate probably due to the planar whole-lung image, in which the surrounding nuclear activity obscures the small focal defect.

Interobserver Variation in Grading of Lung Abnormalities

With use of the 10-point scale, there was general agreement between the reviewers in assessment of the severity of abnormalities. In 17 (53%) of the 32 studies, equal ratings were given by the two reviewers; 30 (94%) of the ratings differed by no more than one point; and in no case did the rating differ by more than two points. There was also a high degree of association between the two reviewers. One reviewer tended to score

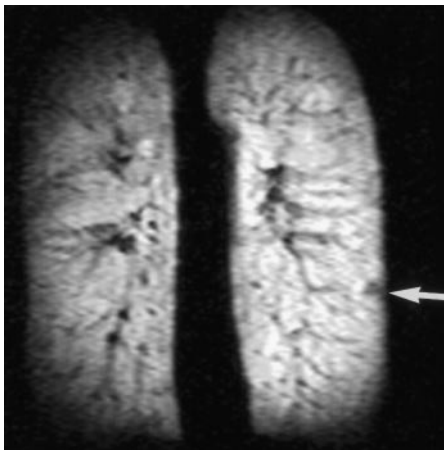

a.

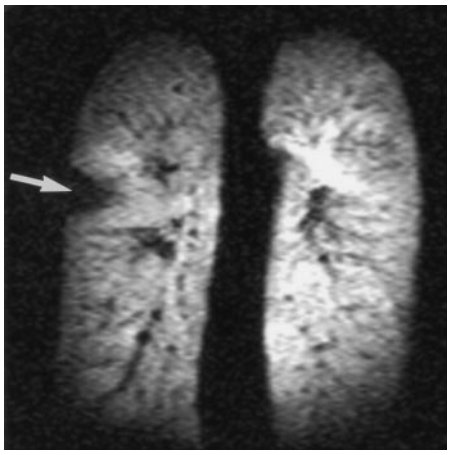

b.

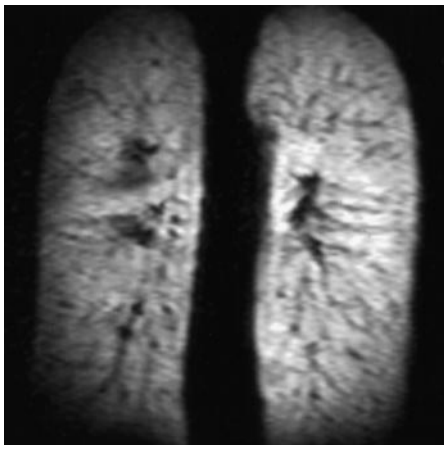

c.

Figure 6. **(a)** Coronal lung ^{3}He image (two-dimensional FLASH) in a 22-year-old healthy subject with mild seasonal allergies and a history of asthma. A very small defect (arrow) but otherwise normal distribution of the gas are seen. **(b)** Follow-up image obtained 1 week later at the same anatomic level demonstrates a new, large defect (arrow) on the right. The small defect on the left has disappeared. **(c)** Repeat follow-up image obtained 1 week after **b** shows that the lungs are normal again.

the abnormalities as slightly more severe than did the other reviewer, but there was little overall difference in the scores. The Spearman rank correlation between the ratings was 0.93, indicating that the ranking of abnormalities on hyperpolarized ^{3}He MR images of the lungs was consistent between the two readers.

Discussion

There are several key differences between noble gas imaging and conventional, hydrogen-based MR techniques. First, the signal in noble gas imaging is provided by the large nonequilibrium nuclear polarization of the gases achieved by means of optical pumping with laser light by using dedicated equipment separate from the MR imager. Thus, the obtained magnetization is independent of the applied magnetic field of the imager. This is in contrast with conventional, hydrogen-based MR imaging, in which the source of the signal is provided by a small fraction of ^{1}H nuclei polarized by the magnetic field of the imager. The magnetization achieved with the laser polarization process is much greater (on the order of 10^{5}) than that for ^{1}H in clinical imagers, allowing the acquisition of images with high signal-to-noise ratios with use of relatively small volumes of gas. Second, when the hyperpolarized gas is used for image acquisition, the magnetization of the gas decreases irreversibly and thus the signal intensity decreases. Thus, with use of the same gas sample, the image quality decreases on subsequent images. This means that if the goal is to obtain multiple image sets of similar signal intensity in the same individual, a fresh sample of polarized gas needs to be inhaled for each image set. This is in contrast to ^{1}H imaging, in which, after each pulse sequence and thus after acquisition of each image set, the polarization of the nuclei returns to the base line (ie, thermal equilibrium) due to the applied magnetic field of the MR imager.

In this study, we found that there was good alveolar distribution of the gas in the majority of cases after a single inhalation and breath hold of the hyperpolarized ^{3}He gas. The images were believed to be of diagnostic quality with good visualization of the air spaces and lung fissures and with very few artifacts from cardiac motion or the pulsating great vessels. Even in the cases with patchy and wedge-shaped ventilation defects, signal intensity from the gas was noted in the periphery of the remaining areas of the lung, indicating that the gas penetration into those areas of the lung was sufficient after a single inhalation. This is not unexpected as helium gas diffuses quickly (approximately 1 mm/msec). In the majority of our studies, imaging was performed with 1 L of 10%–25% hyperpolarized gas; however, no substantial differences in gas distribution were noted in the few cases in which the volume of gas was varied. Although none of our participants experienced any problems inhaling the gas in the volumes provided, it is possible that problems may occur in patients with breathing difficulties. With higher polarizations, however, it is expected that smaller volumes of gas can be used to provide the same imaging results.

In our study, we used a prototypic 28.5-cm Helmholtz coil. For some subjects, this coil was too small, resulting in incomplete coverage of the lungs (Fig 4a). Also, in some cases there was increased signal intensity in the anterior or posterior portions of the lungs due to the proximity of the coil elements to the chest wall or the back (Figs 3b, 3c; 4b). Similar artifacts are also observed frequently with commercial body phased-array coils. Additional limitations of the coil are that it has a linearly polarized design, which does not take advantage of state-of-the-art coil technology such as circularly polarized or phased-array designs.

In a number of our studies, particularly in the ones involving the subjects with a history of smoking, patchy and wedge-shaped ventilation defects were seen. These defects were readily depicted and they were most prominent in the patient with the clinical diagnosis of emphysema. It is most likely that the defects in these cases were based on ventilatory disturbances caused by destruction of lung tissue that typically occurs with smoking. These findings, which have also been observed by others (6,7) performing noble gas MR imaging, are likely to be permanent. Since we did not perform repeat MR imaging in the patients with presumed destructive lung disease, we have no proof that the defects were indeed fixed. In the patient with severe emphysema, however, the fact that similar abnormalities were also seen on the ^{133}Xe wash-in scintigraphic image obtained several months earlier supports the permanent character of the lesions (Fig 5). Findings at ^{133}Xe imaging are usually very reproducible on

repeat studies in patients with emphysema. Transient ventilation defects were also observed in our study, as in our healthy subject with mild seasonal allergies. Although the cause of these defects is unknown, it is likely that they were due to mucous plugging or bronchospasm, processes that are also transient and typically can occur in patients with asthma. The results of our interobserver correlation testing showed that assessment of abnormalities by the two reviewers was performed with only little variation between observers. This suggests that interpretation of the images was reproducible, which is important if this technique is to become clinically useful.

In imaging with hyperpolarized gas, the available magnetization is determined by the gas polarization achieved by the laser process; therefore, there are particular issues with respect to the choice of pulse sequence technique. In fact, hyperpolarized gas imaging is analogous to the situation with magnetization-preparation sequences since the magnetization is obtained independent of and prior to the actual acquisition. Therefore, the use of a low-flip-angle pulse sequence is one straightforward approach to ensure sufficient magnetization is available for all lines in k space. Use of a conventional spin-echo sequence is not appropriate since each 180° pulse would invert the longitudinal magnetization remaining in the image section for the other k-space lines. In addition, because of the many air-tissue interfaces in the lung, susceptibility effects are potentially large, contributing to a short T2* and strongly influencing the appropriate choice of echo time and bandwidth in the sequence for ^{3}He imaging in the lung. However, rapid diffusion of the ^{3}He gas will tend to average these susceptibility gradients on a local level and, therefore, reduce the severity of this constraint.

In the majority of our studies, we used a low-flip-angle, gradient-echo sequence (FLASH) with section-sequential or section-interleaved acquisition, providing sufficient numbers of image sections to cover the lungs in a single 15–22-second breath hold. (We found that a section-sequential, as opposed to section-interleaved, acquisition was beneficial for minimizing motion artifacts from the heart and great vessels. In contrast to conventional proton imaging, the difference in repetition time [13.3 vs 120 msec] between these acquisition modes is irrelevant due to the nature of the hyperpolarized magnetization.) However, since these imaging times may still be relatively long for individuals with breathing difficulties, implementation of faster techniques is crucial. As demonstrated, we evaluated an interleaved, echo-planar, gradient-echo pulse sequence and found that it provides similar quality and the same number of image sections as does the FLASH sequence, but in a much shorter, 5–10-second breath hold.

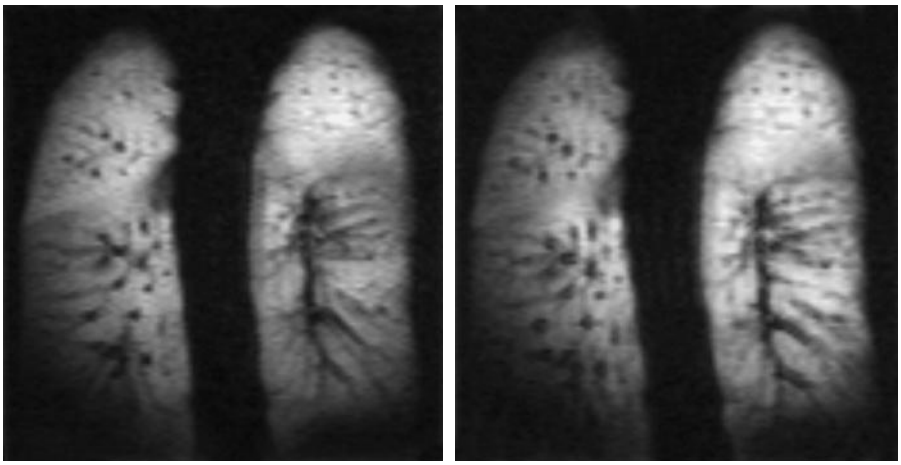

a. **b.**

Figure 7. Coronal **(a)** two-dimensional FLASH image (one of 15 sections obtained in a 20-second breath hold [1.3 seconds per section]) and **(b)** interleaved echo-planar image (one of 15 sections obtained in a 5.7-second breath hold [0.4 seconds per section]) were obtained at approximately the same anatomic level in a healthy subject. Note that the hyperpolarized ^{3}He gas displays similar high signal intensity and there are no substantial differences in diagnostic quality.

Recently, another MR-based technique for depicting lung ventilation has been developed that relies on the paramagnetic properties of molecular oxygen, or O_2, to visualize the lung air spaces (11,12). Hyperpolarized ^{129}Xe has also been used to visualize the air spaces in humans (9). Further development and evaluation of these methods, as well as the method with hyperpolarized ^{3}He, will be required to determine the relative merits of each technique.

In conclusion, with use of hyperpolarized ^{3}He, high-quality lung images can be consistently obtained and ventilatory abnormalities readily depicted, making this technique potentially useful for evaluating pulmonary disease. Hyperpolarized ^{3}He, generated with a compact prototypic polarization system, was used in this study to routinely and reliably produce diagnostic-quality MR images of the air spaces of the lung. The images were rapidly obtained and provided better spatial resolution than is generally possible with ^{133}Xe scintigraphy, currently the most often used ventilation imaging technique. Since MR imaging with hyperpolarized ^{3}He gas has the potential to show the acinar units of the lungs, it is likely that the technique will become particularly useful for evaluating small airways disease such as emphysema, asthma, or cystic fibrosis. However, a limitation is that the gas is relatively expensive (about $100 per liter) due to the limited world supply. Recycling of the ^{3}He gas is likely to reduce the cost. Nevertheless, it is expected that substantial improvements will be possible with further optimization of pulse sequence techniques and coils, providing high-resolution MR images of the lung air spaces with use of smaller gas volumes and shorter acquisition times than were possible in the current study.

Acknowledgments: The authors thank Joe Camaratta, Wilhelm Duerr, PhD, Andreas Potthast, PhD, and Phillip Belcher from Siemens Medical Systems for important contributions in bringing the broad-band imaging-spectroscopy option and the helium radio-frequency coil into operation. From the University of Virginia, we thank Mark R. Conaway, PhD, for performing the statistical analysis, and John Christopher, RT, Shella Keilholz, BS, Therese Maier, MS, and Jaime Mata for valuable assistance with the MR studies.

References

1. Albert MS, Cates GD, Driehuys B, et al. Biological magnetic resonance imaging using laser-polarized ^{129}Xe. Nature 1994; 370:199–201.
2. Middleton H, Black RD, Saam B, et al. MR imaging with hyperpolarized He-3 gas. Magn Reson Med 1995; 33:271–275.
3. Black RD, Middleton HL, Cates GD, et al. In vivo He-3 MR images of guinea pig lungs. Radiology 1996; 199:867–870.
4. Ebert M, Grossmann T, Heil W, et al. Nuclear magnetic resonance imaging with

hyperpolarised helium-3. Lancet 1996; 347:1297–1299.
5. Bachert P, Schad LR, Bock M, et al. Nuclear magnetic resonance imaging of airways in humans with use of hyperpolarized ^{3}He. Magn Reson Med 1996; 36:192–196.
6. Kauczor HU, Hofmann D, Kreitner KF, et al. Normal and abnormal pulmonary ventilation: visualization at hyperpolarized He-3 MR imaging. Radiology 1996; 201: 564–568.
7. MacFall JR, Charles HC, Black RD, et al. Human lung air spaces: potential for MR imaging with hyperpolarized He-3. Radiology 1996; 200:553–558.
8. Kauczor HU, Ebert M, Kreitner KF, et al. Imaging of the lungs using ^{3}He MRI: preliminary clinical experience in 18 patients with and without lung disease. JMRI 1997; 7:538–543.
9. Mugler JP III, Driehuys B, Brookeman JR, et al. MR imaging and spectroscopy using hyperpolarized ^{129}Xe gas: preliminary human results. Magn Reson Med 1997; 37: 809–815.
10. Brookeman JR, Mugler JP III, Bogorad P, et al. Polarized noble gas MRI. In: Polarized gas targets and polarized beams—Seventh International Workshop Conference Proceedings 421 of the American Institute of Physics. Woodburg, NY: Holt & Miller, 1998; 213–217.
11. Edelman RR, Hatabu H, Tadamur E, Li W, Prasad PV. Noninvasive assessment of regional ventilation in the human lung using oxygen-enhanced magnetic resonance imaging. Nat Med 1996; 2:1236–1239.
12. Roberts TP, Kauczor HU, Surkau R, Grossman T, Thelen M. In vivo oxygen tension mapping with helium-3 MR imaging (abstr). Radiology 1997; 205(P):469.